Continuous and Discrete Wavelet Transforms

BM4151 – Biosignal Processing

Nuwan Sriyantha Bandara
180066F

Department of Electronic and Telecommunication Engineering, University of Moratuwa, Sri Lanka

January 10, 2023

Contents

1 Continuous Wavelet Transform

Fourier transform decomposes a signal into linear combinations of complex exponentials of different frequencies and thereby, provides necessary information about the frequencies of the signal. However, it does not include information on the frequency variation with respect to the time domain. In this context, wavelet transform is an approach to attain both frequency information and respective time information of a given signal with all resolutions.

The continuous wavelet transform (CWT) is defined as below:

$$W(s,\tau) = \int x(t)\frac{1}{\sqrt{s}}\psi(\frac{t-\tau}{s})\,dt \tag{1}$$

where s is the scaling factor, τ and ψ are translation and wavelet function respectively.

1.1 Wavelet properties

Derivation of Mexican hat function Let the Gaussian function be $g(t)$ and Mexican hat function be $m(t)$, then,

$$m(t) = -\frac{d^2g(t)}{dt^2} \tag{2}$$

where, with $\mu = 0$ and $\sigma^2 = 1$,

$$g(t) = \frac{1}{\sqrt{2\pi}}e^{-0.5t^2} \tag{3}$$

$$\frac{dg(t)}{dt} = \frac{-t}{\sqrt{2\pi}}e^{-0.5t^2}$$

$$\frac{d^2g(t)}{dt^2} = \frac{t^2}{\sqrt{2\pi}}e^{-0.5t^2} + \frac{-1}{\sqrt{2\pi}}e^{-0.5t^2}$$

Therefore,

$$m(t) = \frac{(1-t^2)}{\sqrt{2\pi}}e^{-0.5t^2} \tag{4}$$

The normalizing factor of $m(t)$ calculation:

$$E = \int_{-\infty}^{\infty}[m(t)]^2\,dt \tag{5}$$

$$E = \int_{-\infty}^{\infty}\frac{(t^2-1)^2 \times e^{-t^2}}{2\pi}\,dt$$

$$E = \Big[\frac{3erf(t)}{10\pi} - \frac{t(2t^2-1)e^{-t^2}}{81}\Big]_{-\infty}^{\infty}$$

where $erf(z)$ is the error function defined as:

$$erf(z) = \frac{2}{\sqrt{\pi}}\int_0^z e^{-t^2}\,dt \tag{6}$$

Therefore,

$$E = \frac{3}{8\sqrt{\pi}} \tag{7}$$

However, the energy of the Mexican hat wavelet function must be equal to 1 and thus, the unity energy could be attained by normalizing the Mexican hat function through the following normalization factor $1/\sqrt{E}$:

$$\frac{1}{\sqrt{E}} = \sqrt{\frac{8\sqrt{\pi}}{3}} \tag{8}$$

Therefore, the normalized Mexican hat wavelet, $m_{norm}(t)$, could be defined as:

$$m_{norm}(t) = \frac{1}{\sqrt{E}} m(t) \tag{9}$$

$$m_{norm}(t) = \frac{2\sqrt{2}\pi^{0.25}}{\sqrt{3}} \times \frac{(1-t^2)}{\sqrt{2\pi}} e^{-0.5t^2}$$

$$m_{norm}(t) = \frac{2(1-t^2)}{\sqrt{3}\pi^{0.25}} e^{-0.5t^2}$$

Therefore, the normalized Mexican hat mother wavelet could be derived as:

$$\psi_{s,\tau}(t) = \frac{1}{\sqrt{s}} \psi(\frac{t-\tau}{s}) \tag{10}$$

$$\psi_{s,\tau}(t) = \frac{2}{\sqrt{3s}\pi^{0.25}} \left[1 - (\frac{t-\tau}{s})^2\right] e^{-0.5(\frac{t-\tau}{s})^2} \tag{11}$$

Since wavelets have zero means, unity energies while being limited in the time domain, through $m(t)$, it is observable that the $m(t)$ is approximately zero for both vary large and small t values which indicates the applicability of Mexican hat function as a valid wavelet. Further, this implies that the function is practically a time-limited signal and thus, has compact support.

Daughter wavelets of the Mexican hat wavelet with scaling factors of 0.01 to 2 with 0.1 time intervals are resented in the below figure.

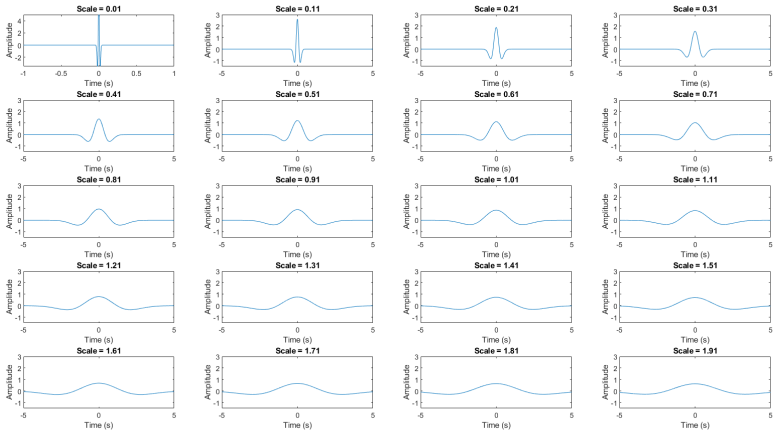

Figure 1: Daughter wavelets for Mexican hat wavelet for a set of scaling factors from 0.01 to 2 with 0.1 intervals

In accordance with Figure 1, it is observable that all daughter wavelets of the Mexican hat wavelet are limited in the time domain and thus, it is verifiable the compact support of the daughter wavelets.

Through figure 2, it is conveyed that all daughter wavelets have zero means and unity energies with them.

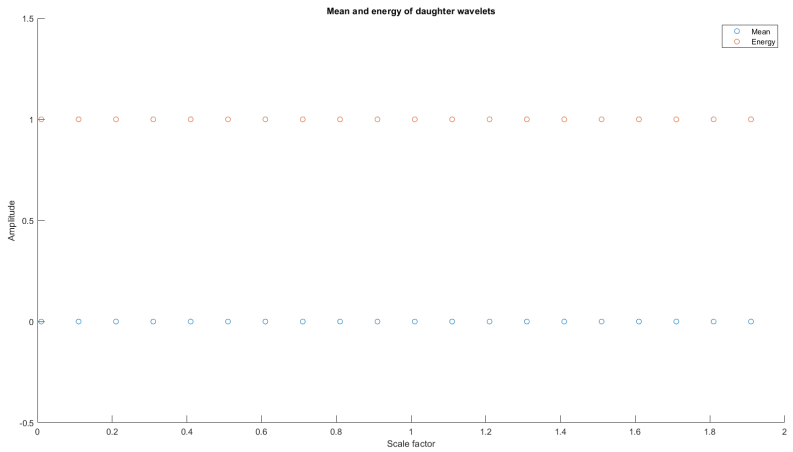

Figure 2: Mean and energy of daughter wavelets of Mexican hat mother wavelets for the same defined set of scaling factors

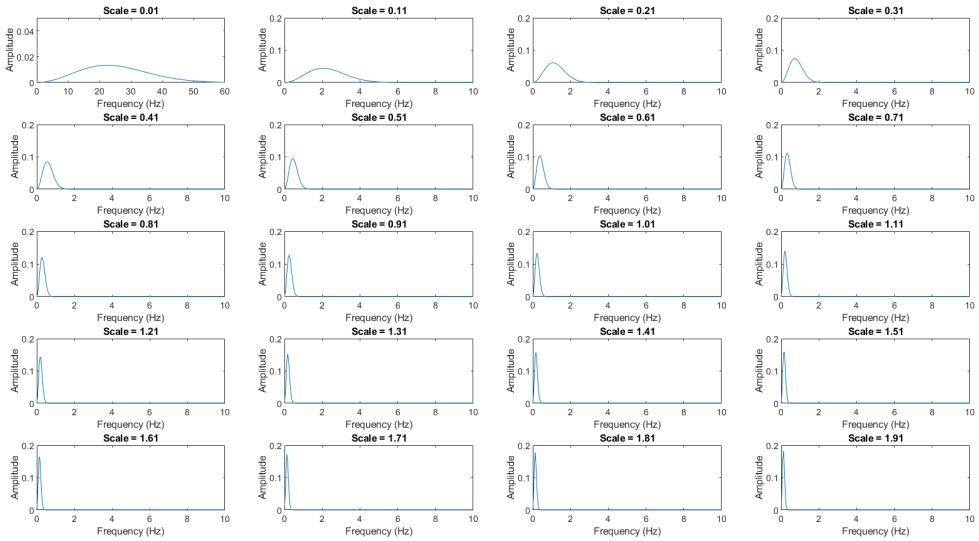

Figure 3: Frequency spectra of daughter wavelets of Mexican hat mother wavelet for the same defined set of scaling factors

Through figure 3, it could be deduced that the daughter wavelets have bandpass characteristics in the frequency domain in which the centre frequency of the pass-band depends on the scaling factor. More specifically, the centre frequency is higher at lower

scaling factors and it gradually decreases with the increment of the scaling factor. This behaviour implies that the small scaling factors have the potential to capture higher frequency components of the given signal more effectively.

1.2 Continuous Wavelet Decomposition (CWD)

The continuous waveform is attained using the following equation for this experiment.

$$x[n] = \begin{cases} sin(0.5\pi n) & 1 \leq n < \frac{3N}{2} \\ sin(1.5\pi n) & \frac{3N}{2} \leq n < 3N \end{cases} \tag{12}$$

Since the bandwidth of the daughter wavelets decreases with the scaling factor increment (as observed in figure 3), it is observable in figure 5 that the wavelets with higher scaling factors capture lower frequencies in the signal while the wavelets with lower scaling factors effectively capture the higher frequency components in the signal.

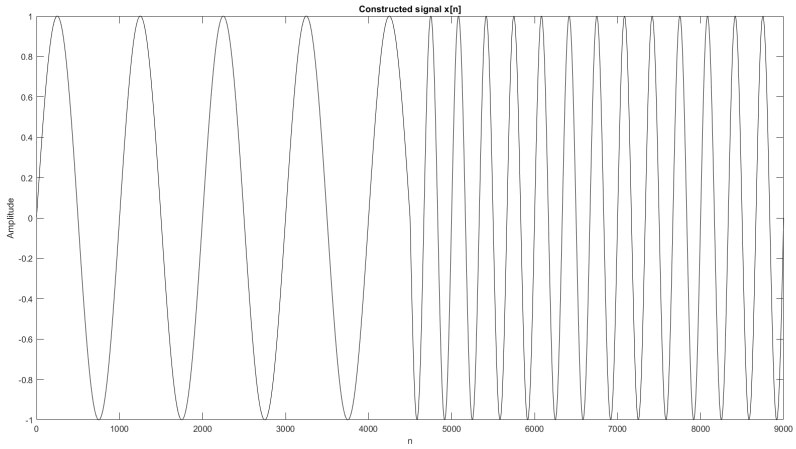

Figure 4: $x[n]$ waveform visualization

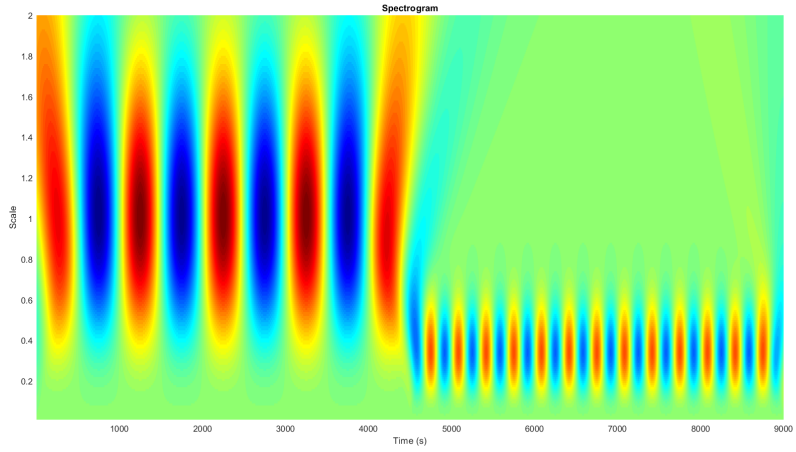

Figure 5: Frequency spectrum of derived CWT coefficients

In addition, it could be perceived that the wavelets with a scaling factor near 1 have their centre frequency near $0.5\pi\, rads^{-1}$ while the wavelets with scaling factor near 0.31 have their centre frequency near $1.5\pi\, rads^{-1}$. Therefore, those frequency parts of the signals are highlighted in the spectrogram whereas, for other scaling factors, the spectrogram representation is low. Hence, it can deduce that the continuous wavelet transform represents the frequency spectrum and the respective time-domain frequency variation of the signal with sufficient accuracy we derived from the theoretical equations.

2 Discrete Wavelet Transform

The discrete wavelet transform (DWT) decomposes a given signal into a defined number of sets in which each set is a time series of coefficients corresponding to the temporal evolution of the signal in the respective frequency band. In addition, DWT considerably eliminates the drawback of CWT: highly redundant computations leading to the requirement of additional computational power and time consumption, by utilizing the discrete scaling factors.

The DWT is defined in the following equation:

$$\psi_{m,n}(t) = \frac{1}{\sqrt{s_0^m}}\psi\Big(\frac{t - n\tau_0 s_0^m}{s_0^m}\Big) \tag{13}$$

where s_0, τ_0, m and n are scaling step size, translation step size and corresponding multiplier integers respectively.

2.1 Application of DWT with the Wavelet Toolbox

Given that $s_0 = 2$ and $\tau_0 = 1$ for this experiment, the following waveforms are utilized.

$$x_1[n] = \begin{cases} 2sin(20\pi n) + sin(80\pi n) & 0 \leq n < 512 \\ 0.5sin(40\pi n) + sin(60\pi n) & 512 \leq n < 1024 \end{cases} \tag{14}$$

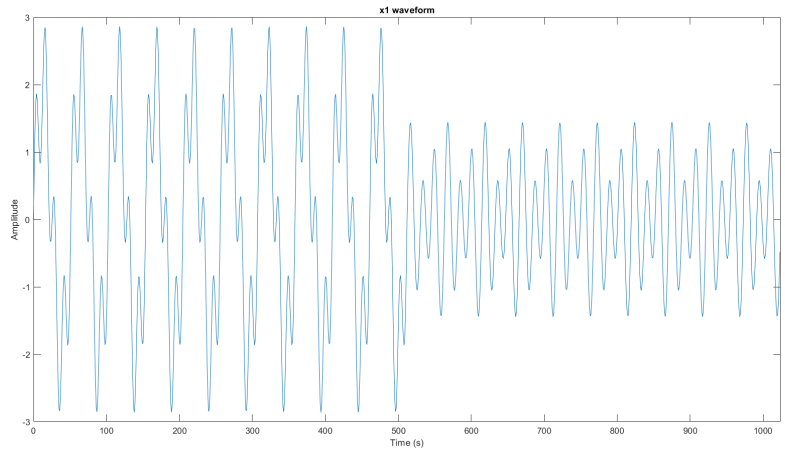

Figure 6: $x_1[n]$ waveform visualization

$$x_2[n] = \begin{cases} 1 & 0 \leq n < 64 \\ 2 & 192 \leq n < 256 \\ -1 & 256 \leq n < 512 \\ 3 & 512 \leq n < 704 \\ 1 & 704 \leq n < 960 \\ 0 & otherwise \end{cases} \tag{15}$$

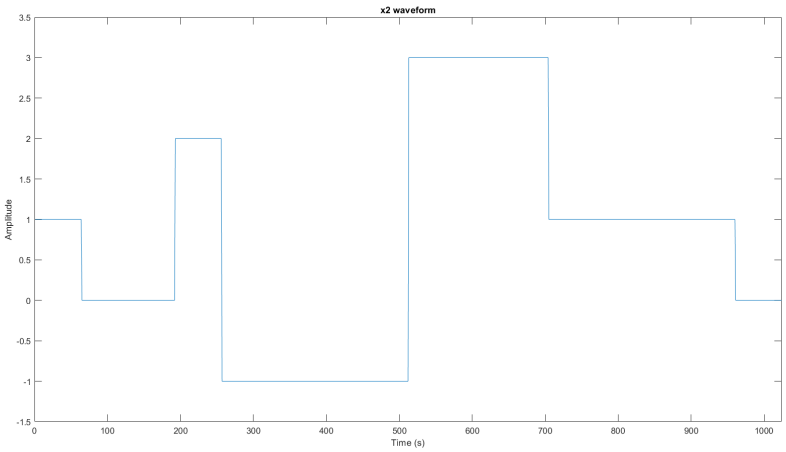

Figure 7: $x_2[n]$ waveform visualization

Afterwards, corresponding noisy signals, $y_1[n]$ and $y_2[n]$, were obtained by adding $10dB$ white Gaussian noise to the signals, $x_1[n]$ and $x_2[n]$, respectively. DWT is applied to the above two noisy signals with wavelet functions: Haar wavelet and Daubechies 9-tap (db9).

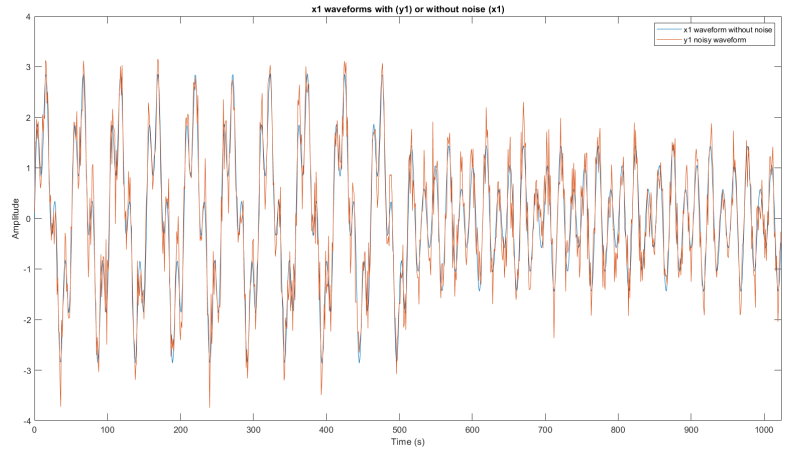

Figure 8: $y_1[n]$ (noisy $x_1[n]$) waveform visualization

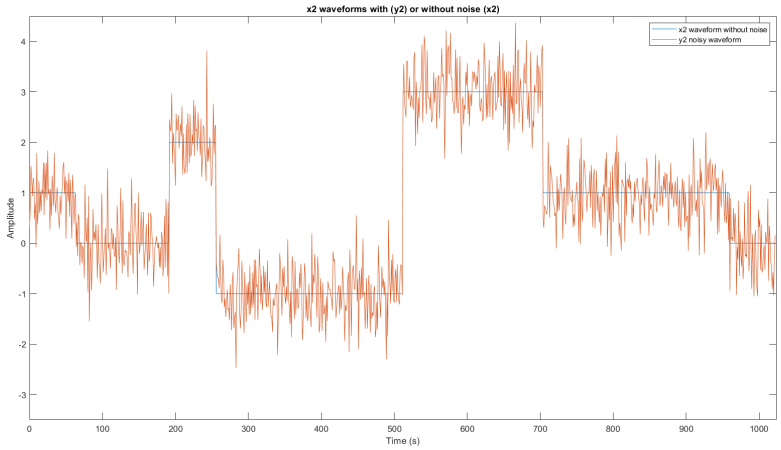

Figure 9: $y_2[n]$ (noisy $x_2[n]$) waveform visualization

Wavelet observation The *waveletAnalyzer* tool is utilized to observe the properties of Harr and db9 wavelets.

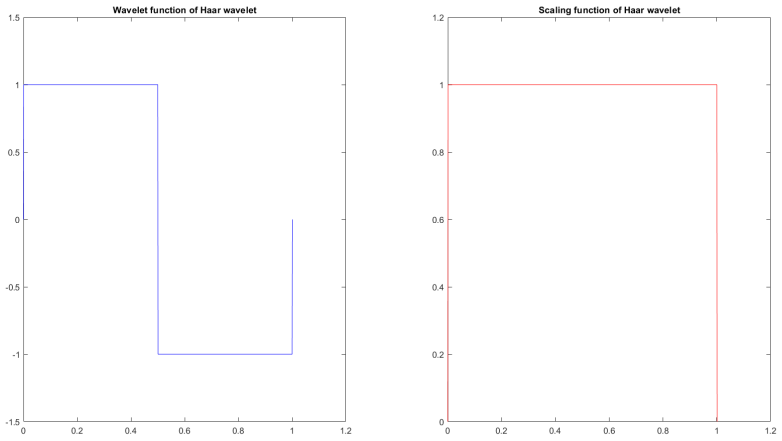

Figure 10: Wavelet and scaling functions of Haar wavelet

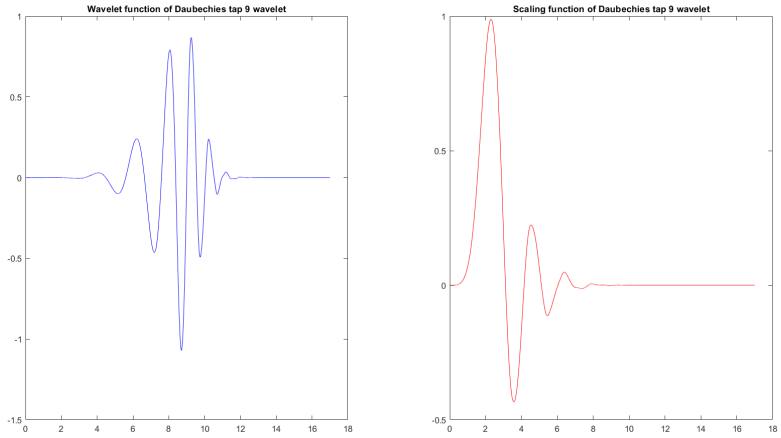

Figure 11: Wavelet and scaling functions of db9 wavelet

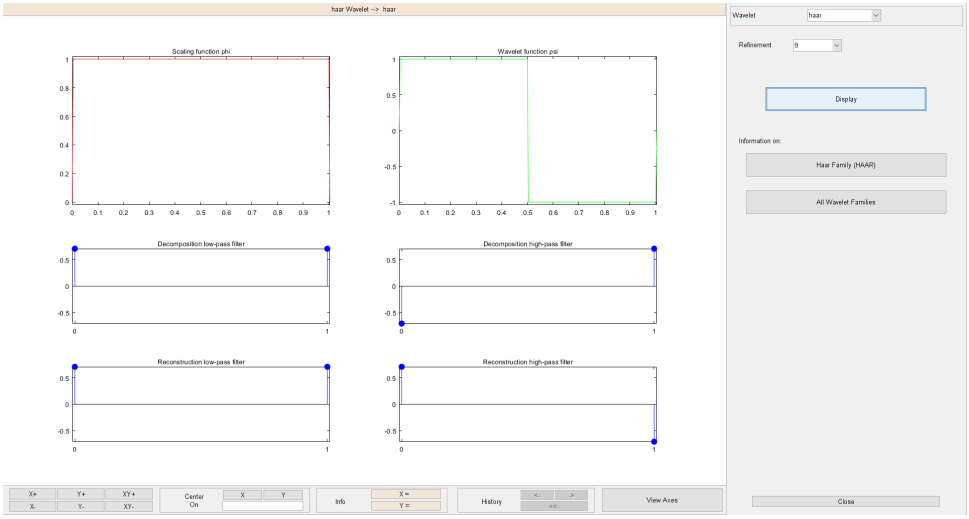

Figure 12: Wavelet properties of Haar wavelet from *waveletAnalyzer*

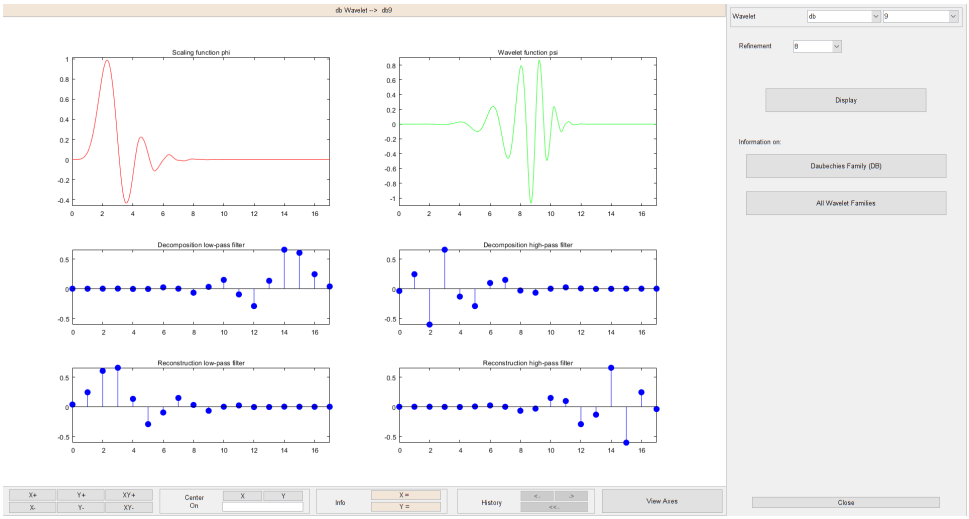

Figure 13: Wavelet properties of db9 wavelet from *waveletAnalyzer*

Wavelet decomposition Since the signal has 1024 samples, the maximum number of dyadic wavelet decompositions to be applied could be calculated as:

$$log_2(1024) = 10 \tag{16}$$

Afterwards, wavelet decomposition is executed for both y_1 and y_2 noisy signals with both wavelet functions.

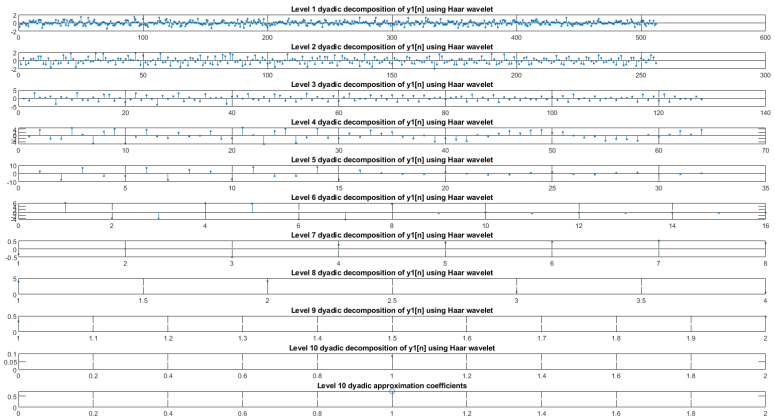

Figure 14: $y_1[n]$ decomposition using Haar wavelet

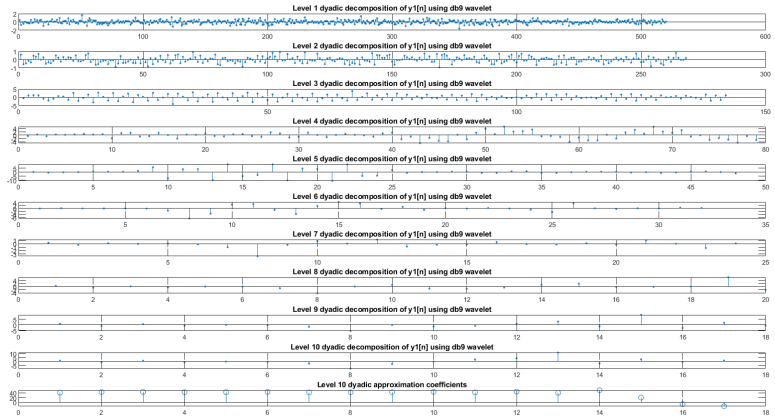

Figure 15: $y_1[n]$ decomposition using db9 wavelet

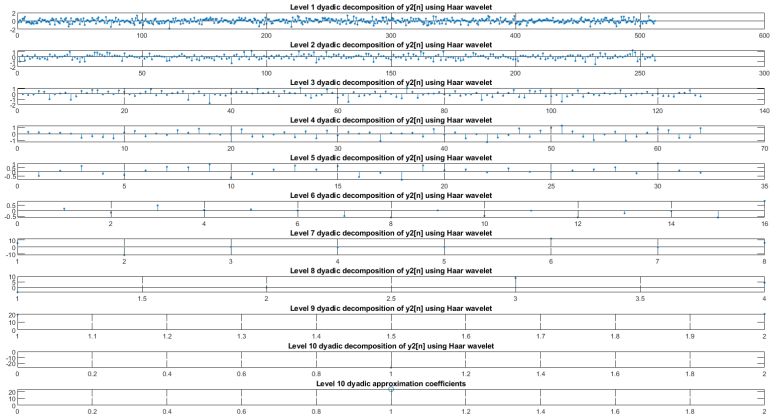

Figure 16: $y_2[n]$ decomposition using Haar wavelet

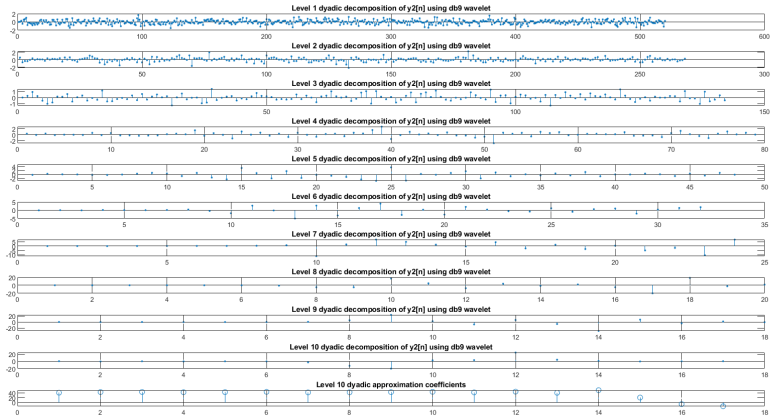

Figure 17: $y_2[n]$ decomposition using db9 wavelet

Wavelet reconstruction The signal can be reconstructed using the detailed function coefficients and the approximation function coefficients of the respective wavelet (in accordance with the number of decomposing levels). The similarity of the reconstructed signal and the original signal could be calculated using the root mean square error (RMSE) between the two signals.

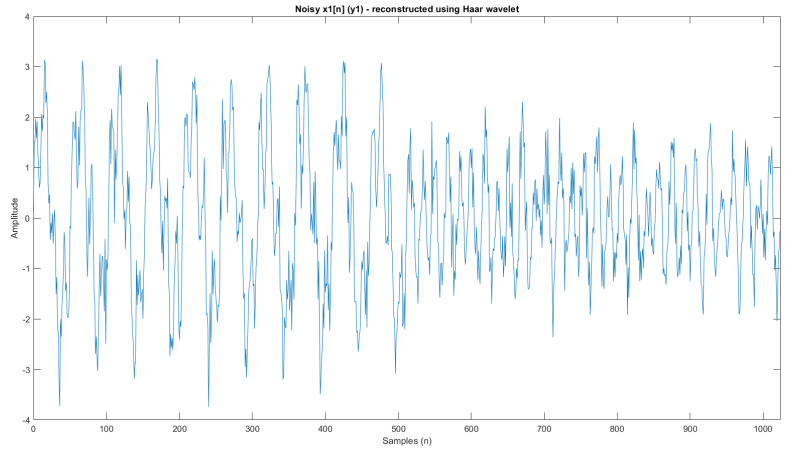

Figure 18: $y_1[n]$ (noisy $x_1[n]$) reconstruction using Haar wavelet

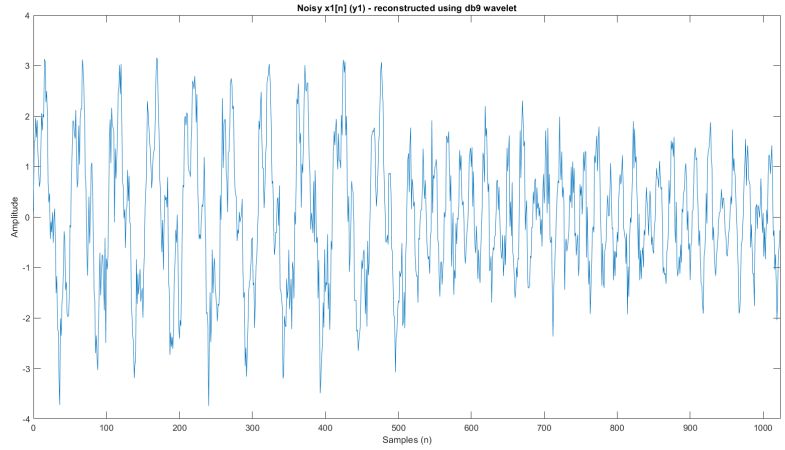

Figure 19: $y_1[n]$ (noisy $x_1[n]$) reconstruction using db9 wavelet

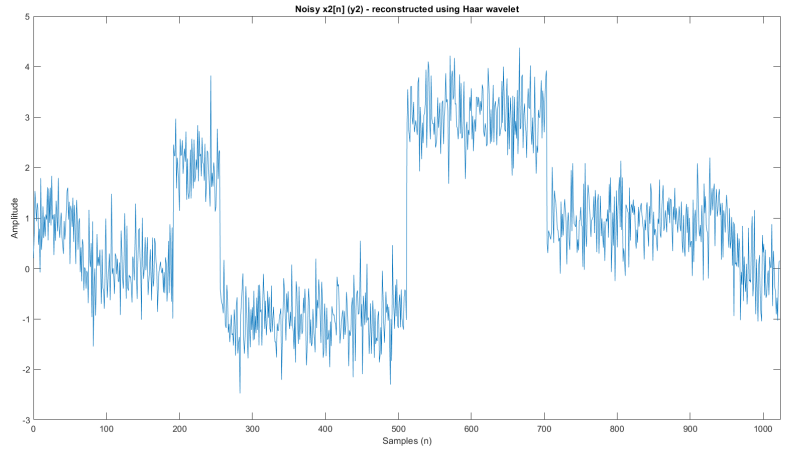

Figure 20: $y_2[n]$ (noisy $x_2[n]$) reconstruction using Haar wavelet

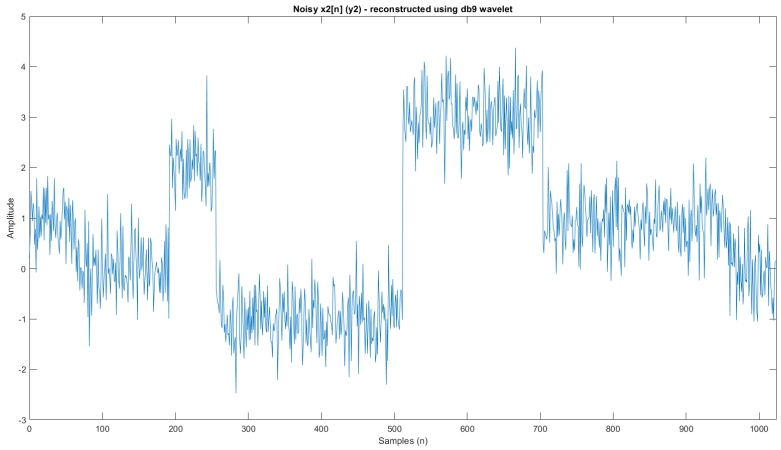

Figure 21: $y_2[n]$ (noisy $x_2[n]$) reconstruction using db9 wavelet

	$y_1[n]$	$y_2[n]$
Original signal energy	1734.216899751	2844.859163948
The energy of the reconstructed signal with Haar	1734.216899751	2844.859163948
The energy of the reconstructed signal with db9	1734.216899454	2844.859163514

Table 1: Energy comparison between original and reconstructed signals

2.2 Signal Denoising with DWT

A set of detailed coefficients at different translations for each scale for the signal was obtained through wavelet decomposition and it is sensible to neglect certain features through the removal of a set of selected coefficients (the selection is made through a threshold in which if a coefficient is lower than the set threshold, then it is considered to be noise and thus, to be removed) by setting them into zero and afterwards, perform the wavelet reconstruction. Here, the threshold for signal denoising is selected by observing the coefficients through each wavelet type.

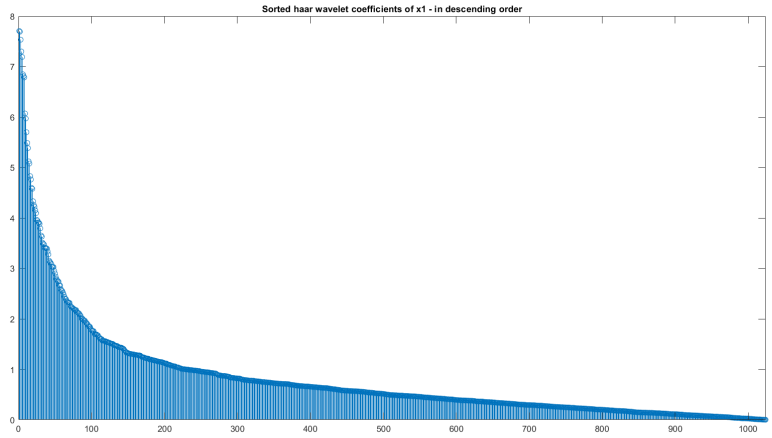

Figure 22: Sorted Haar wavelet coefficients of noisy $x_1[n]$ in the descending order

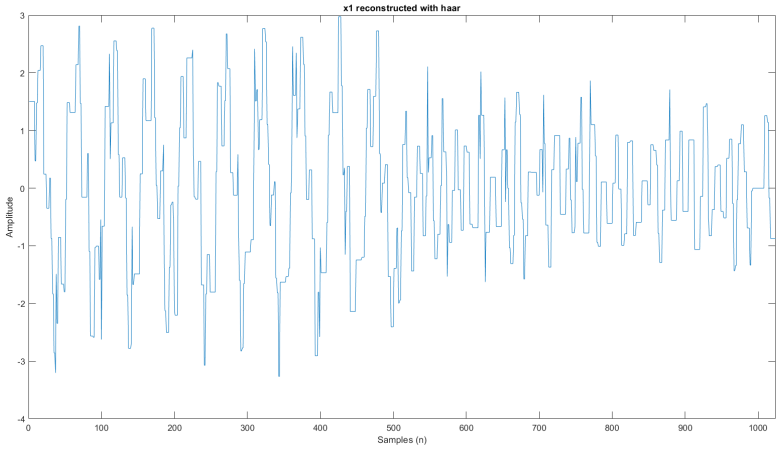

Figure 23: Reconstructed $x_1[n]$ with thresholded coefficients using Haar wavelet

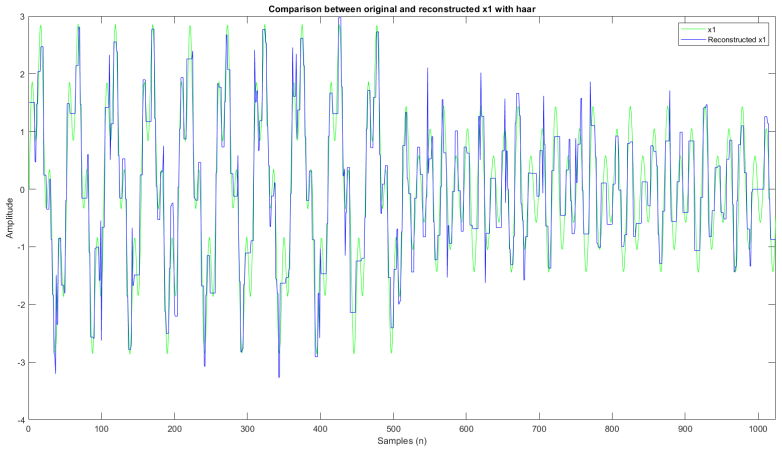

Figure 24: Comparison of original and denoised $x_1[n]$ using Haar wavelet

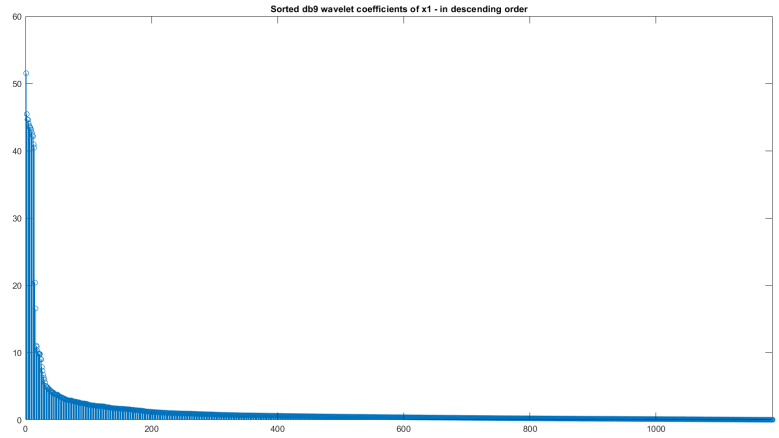

Figure 25: Sorted db9 wavelet coefficients of noisy $x_1[n]$ in the descending order

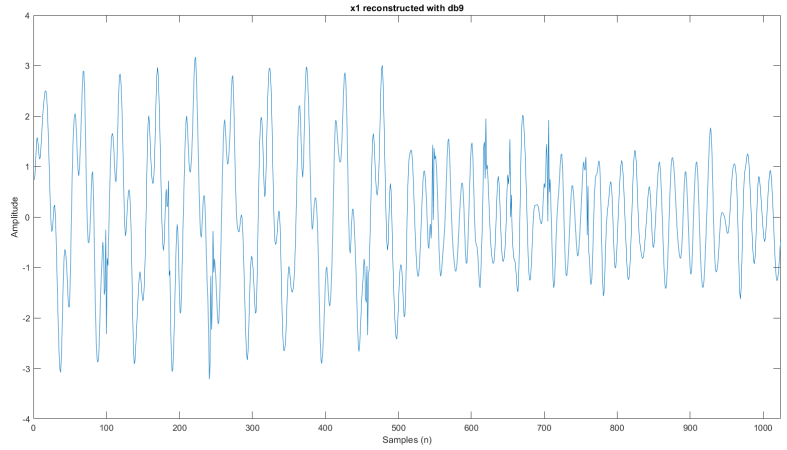

Figure 26: Reconstructed $x_1[n]$ with thresholded coefficients using db9 wavelet

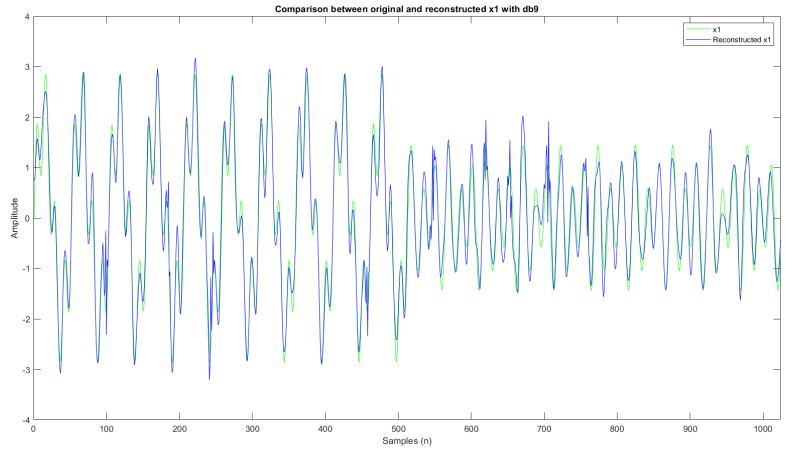

Figure 27: Comparison of original and denoised $x_1[n]$ using db9 wavelet

Wavelet transforms were applied to $y_2[n]$ and to the denoised signal as well.

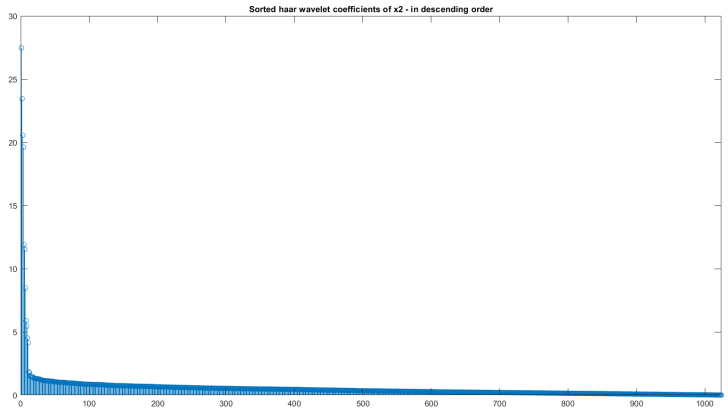

Figure 28: Sorted Haar wavelet coefficients of noisy $x_2[n]$ in the descending order

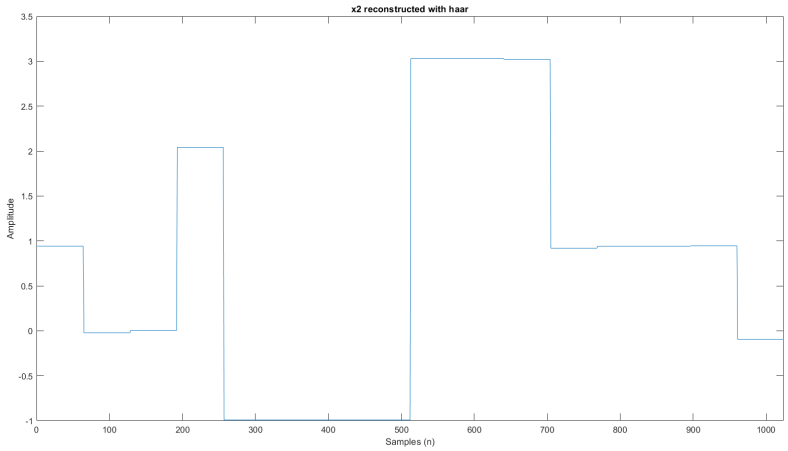

Figure 29: Reconstructed $x_2[n]$ with thresholded coefficients using Haar wavelet

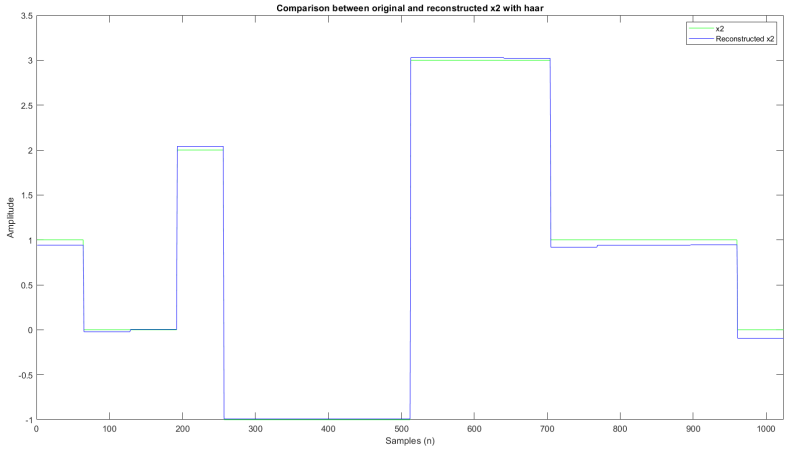

Figure 30: Comparison of original and denoised $x_2[n]$ using Haar wavelet

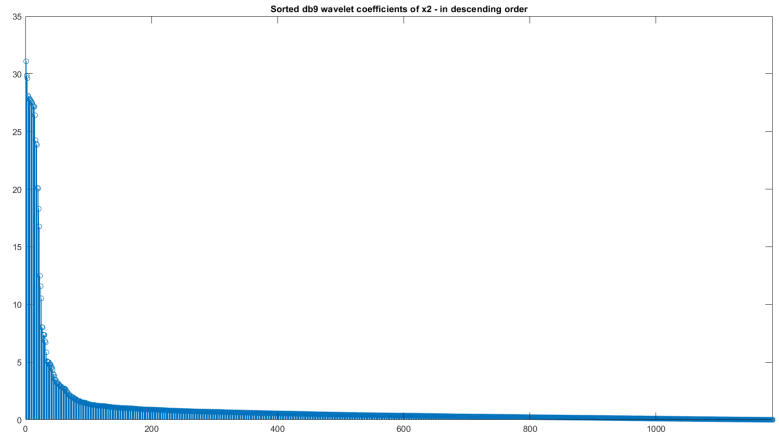

Figure 31: Sorted db9 wavelet coefficients of noisy $x_2[n]$ in the descending order

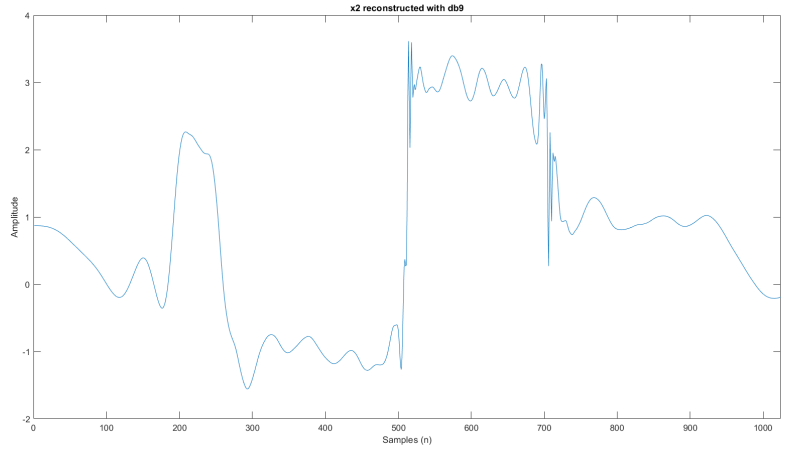

Figure 32: Reconstructed $x_2[n]$ with thresholded coefficients using db9 wavelet

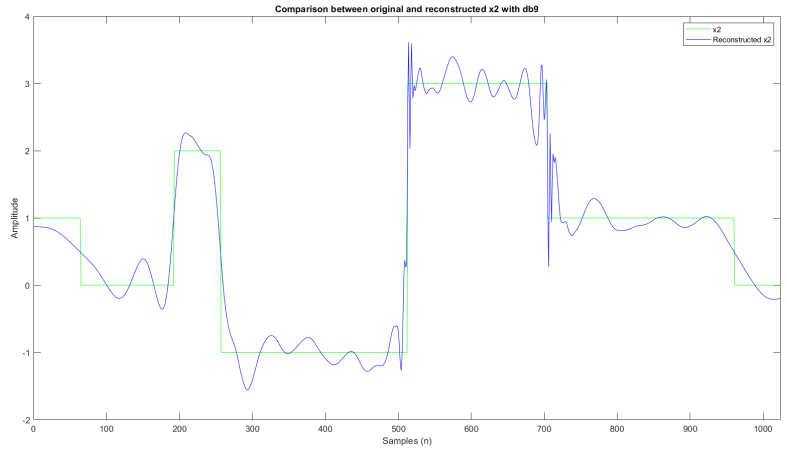

Figure 33: Comparison of original and denoised $x_2[n]$ using db9 wavelet

Signal	Wavelet	Threshold	RMSE
$y_1[n]$	Haar	1	0.43689
	db9	1	0.27533
$y_2[n]$	Haar	2	0.050483
	db9	2	0.26837

Table 2: Comparison of RMSE values with different thresholds and wavelets in denoising

Through the RMSE results, it could be deduced that the signals with rapid transitions (as $y_2[n]$) can be denoised using the Haar wavelet with superior performance than using Daubechies wavelet since the RMSE for Haar wavelet is lower (i.e. a better fit to the original signal) in compared to db9. However, through $y_1[n]$, it could be shown that the signals with sinusoidal variations could be denoised using db9 with better performance, compared to Haar when considering the RMSE values and plots.

2.3 Signal compression with DWT

Wavelet coefficients, which are defined to be "very small", could be neglected by considering them as added noise to the original signal and thereby, having a minimal contribution to the signal. In signal compression, wavelet coefficients are considered to be kept until those components collectively preserve the given percentage of energy. In contrast, other non-contributory components are removed by setting their values to zero. Here, aV_R lead ECG raw signal is loaded for the signal compression and the sampling frequency is set to be $257Hz$ and two wavelet transforms are applied. Here, the maximum number of dyadic wavelet decomposition which could be applied is equal to:

$$log_2(2570) \approx 12 \tag{17}$$

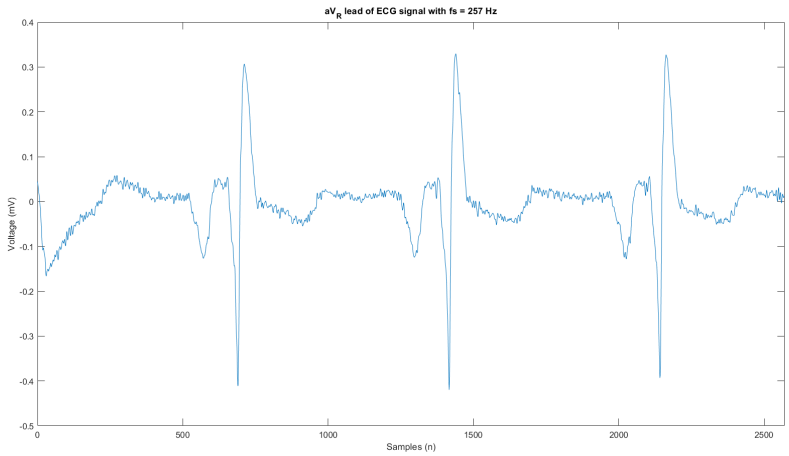

Figure 34: aV_R lead ECG waveform with $fs = 257Hz$

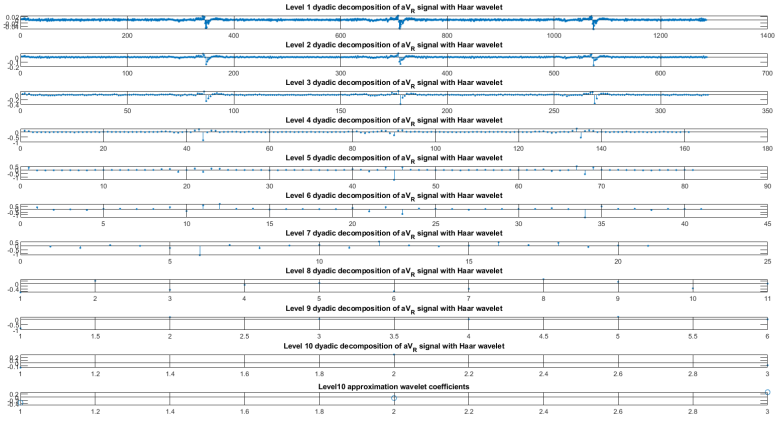

Figure 35: Wavelet Decomposition of aV_R lead ECG signal using Haar wavelet

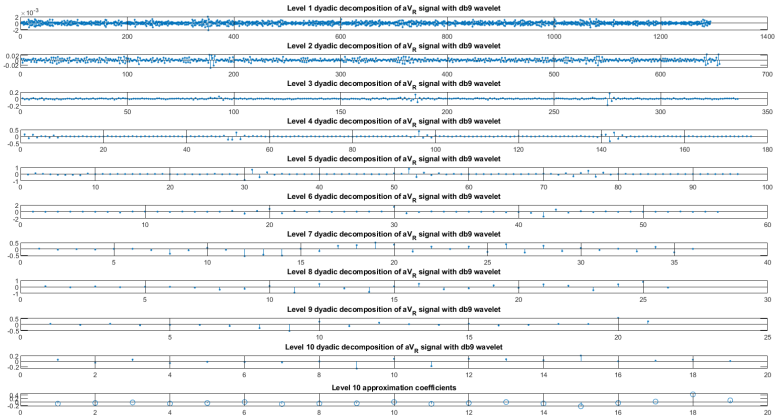

Figure 36: Wavelet Decomposition of aV_R lead ECG signal using db9 wavelet

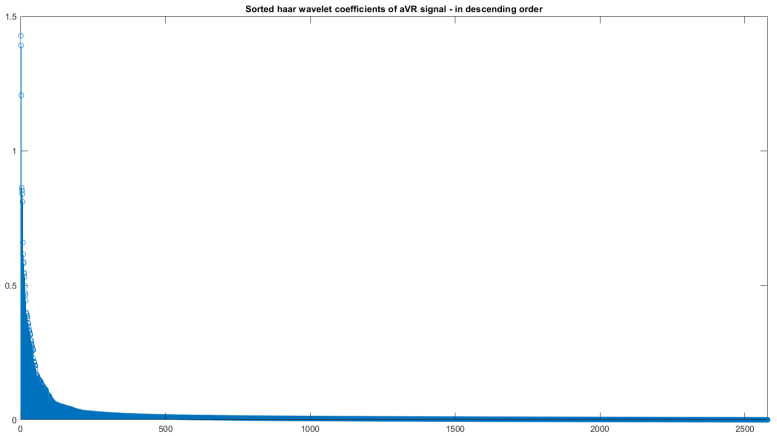

Figure 37: Sorted Haar wavelet coefficients of aV_R ECG signal in descending order

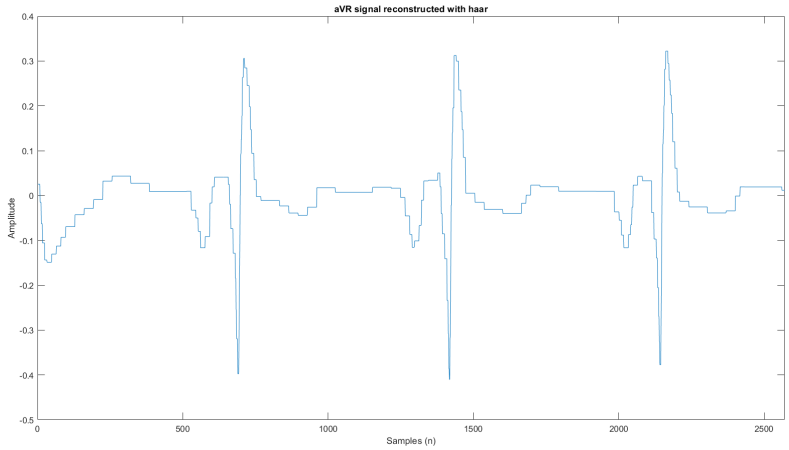

Figure 38: aV_R signal reconstructed with Haar wavelet

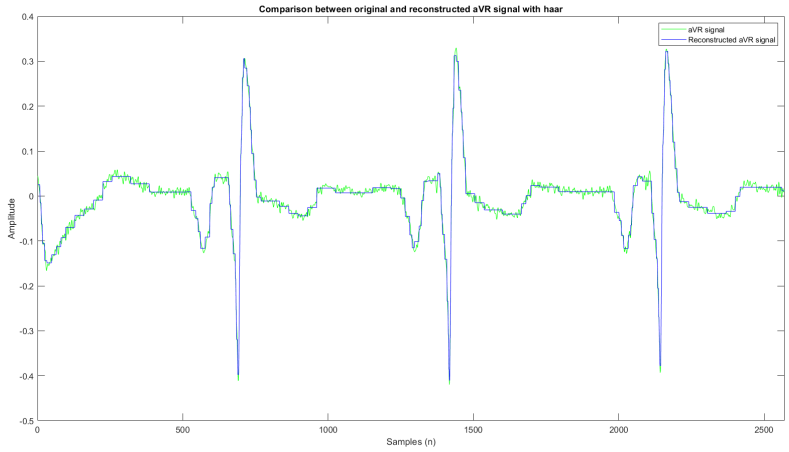

Figure 39: Comparison between original and reconstructed aV_R ECG signal with Haar wavelet

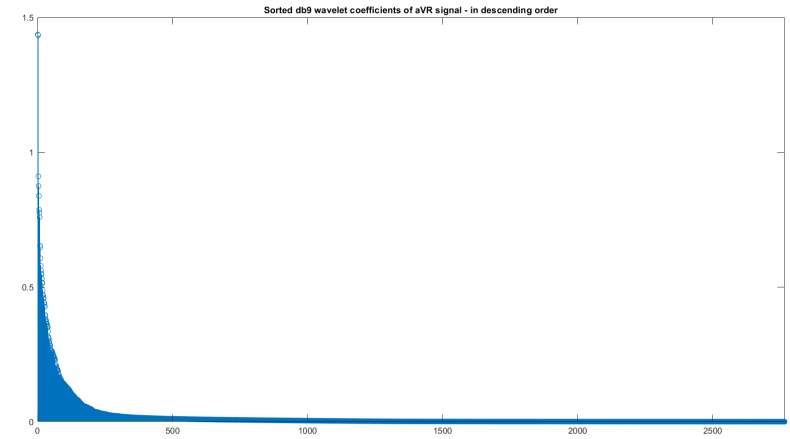

Figure 40: Sorted db9 wavelet coefficients of aV_R ECG signal in descending order

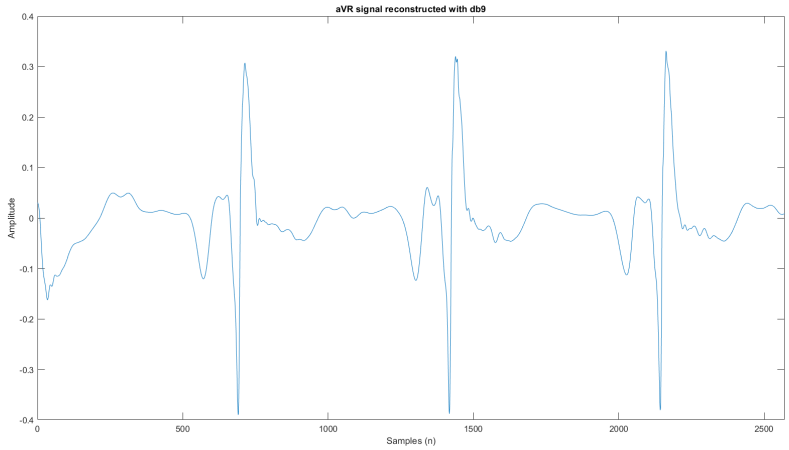

Figure 41: aV_R signal reconstructed with db9 wavelet

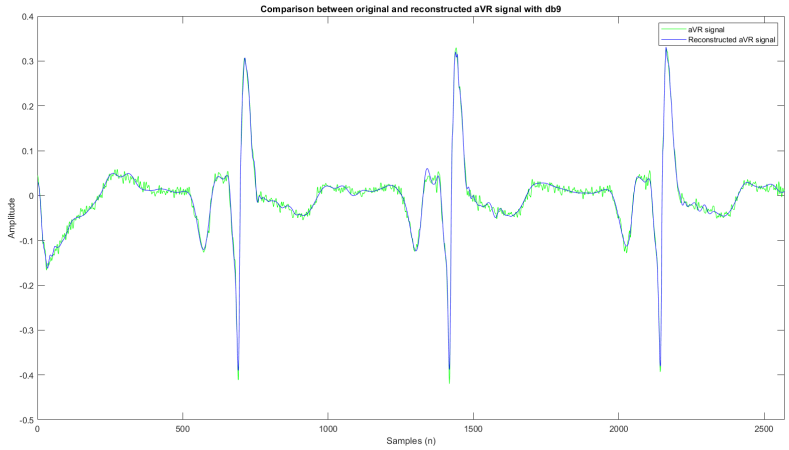

Figure 42: Comparison between original and reconstructed aV_R ECG signal with db9 wavelet

Here, the compression ratio (CR) is defined as:

$$CR = \frac{signal\ length}{selected\ signal\ coefficients} \tag{18}$$

Wavelet	Energy Percentage	No of coefficients needed	Compression Ratio	RMSE
Haar	99%	138	18.6232	0.0095818
Db9	99%	161	15.9627	0.0081062

Table 3: Comparison of the number of coefficients needed, compression ratio, and RMSE using two wavelets

Through the results, it could be perceived that the compression using Haar is better than in the db9 wavelet and thus, Haar is able to reconstruct the signal with 99% energy

with lesser coefficients than to db9 wavelet. This shows that even though the Haar wavelet has sharp edges and thus, it can not properly approximate the smoothing shapes of the ECG signal, it can easily achieve the required energy approximation in comparison to db9. However, it is further to be noted that with a higher compression ratio, the RMSE of Haar is also slightly higher than that of db9 which is a disadvantage of using Haar.